NTNU
Innovation and Creativity

Ultrasound Examination of Steel Pipes

Anders Driveklepp

Master of Science in Electronics
Submission date: June 2007
Supervisor: Odd Kr. Pettersen, IET
Co-supervisor: Tor Arne Reinen, SINTEF

Norwegian University of Science and Technology
Department of Electronics and Telecommunications

Problem Description

The assignment is to carry out introductory examinations of the possibilities for the use of ultrasound transducers for examination of oil pipelines. Experimental work should be carried out in order to investigate the possibilities of diagnosing flaws in steel pipes by using ultrasound and signal processing.

Assignment given: 15. January 2007
Supervisor: Odd Kr. Pettersen, IET

Preface

This master thesis is the result of an experimental work in the field of vibroacoustics. The work was carried out in the period January-June 2007, at the Department of Electronics and Telecommunications at the Norwegian University of Science and Technology, and serves as a part of the early research for the SmartPipe project led by SINTEF, Trondheim.

There are several people who should be thanked for making this thesis become what it is. I have tried to thank them every time they have helped me, but some of them must be mentioned here anyway. First of all, I would like to thank my project supervisor, senior scientist at SINTEF, Tor Arne Reinen for our weekly meetings, for his patience and for his support and invaluable guidance throughout the project. Thank you also to the project main supervisor, research director at SINTEF, prof. II at NUST, Odd K Østern Pettersen, for assigning me to the project, and for constructive input.

I also want to thank Øyvind Lervik, Tone Berg, the people from the workshop in the telecommunications department, my brother Pål and the guys at Omega Verksted.

Anders Driveklepp

Gløshaugen, Trondheim, 15th of June 2007

Abstract

Non-intrusive testing of pipelines has become a growing industry, and is expected to keep growing as the demands on quality control and safety keep increasing. In order to meet the oil industry's demands for pipe monitoring of sub sea pipelines, the SmartPipe project was initiated by SINTEF in Trondheim, Norway. One of the primary objectives of the SmartPipe project is develop a system for in-service monitoring of the pipelines that are placed on the seabed by the offshore oil industry.

This thesis presents a very early step in the research required for the development of such a system. The purpose of the presented work was to carry out introductory experimental work in order to find out whether it is possible to develop relatively simple techniques for in-service testing of sub sea steel pipes. A so-called pitch-catch setup and various wedges was used in order to test the area between a pair of 5 MHz ultrasound transducers. Measuring over a distance of 1.00 m, rather than just single points on the pipe, could provide more general information about the condition of the pipe. Tests with over 4 m distance between transducers were also carried out.

Measurement stability and mechanical coupling are of crucial importance in ultrasonic test systems, and useful knowledge on the subjects has been gained and are documented in this thesis. Results from measurements indicate that comprehensible results can be attained even with very simple measurement setups. Especially when using special wedges for introduction of Rayleigh waves, the received signals had high amplitudes and the signal envelope had a simple shape. The effect that the damage to the pipe had on the Rayleigh waves, was found to be equally simple and predictable. Shear waves and longitudinal waves that are less sensitive to the surrounding medium, were also shown to be applicable in flaw detection. Results and discussion include both time domain, frequency domain and energy considerations.

Keywords: Rayleigh waves, angle-beam wedges, mechanical coupling, mode conversion

II

Contents

1 Introduction

Every year vast amounts of pipelines are constructed and put into service. According to a website [SmartPipe] by SINTEF, between 50000 and 100000 km of new pipelines are planned for the next five years. Many of these are exposed to extremely harsh environments that require high quality and quality control. One example of such pipes is the oil and gas pipelines that connect offshore installations with the shore. Monitoring of such pipelines would be favourable both for environmental safety aspects and for financial and logistical purposes. In recent years an increasing number of solutions for non-intrusive testing has become commercially available, but these are often not suitable for inaccessible locations such as the seabed.

Systems for point monitoring of pipe wall thickness do exist, but measuring the thickness in a few positions is not really enough to assess the overall condition of a pipe. Therefore it is of great interest to the SmartPipe project at SINTEF to look into the possibilities for the development of a system with transducers that are able to monitor sections of the pipe, rather than just selected points. The SmartPipe project is a research project initiated by SINTEF in Trondheim. Oil companies, local industry and the Norwegian University of Science and Technology are partners involved in the project. In short terms the aim of the SmartPipe project is to develop a complete pipe monitoring system that is an integrated part of the pipeline. Sensors are planned to monitor both parameters such as the flow inside the pipes and temperature, but also the condition of the pipe itself.

Theoretical analysis of wave propagation in pipe walls, and the phenomena associated with anomalies in such geometries, are rather complicated and are today at the front of modern research. This thesis has its focus on experimental work, and is not a study of the theoretical aspects of these phenomena. Instead, relatively simple high frequency methods will be applied and evaluated. This choice is motivated by the need for small and simple sensors and systems for the SmartPipe project.

Because this master thesis was undertaken at a very early stage in the SmartPipe project at SINTEF, it does not contain practical solutions for a pipe monitoring system. Instead it is meant to provide information that will hopefully give an indication of the possibilities for further development of such a system. Since SINTEF is probably going to do further work on ultrasound testing of steel pipes, this thesis is also meant to document some of the practical measurement techniques that were learned during the experimental work.

The thesis has a brief theory part (section 2) where basic theory about

wave types, mode conversion, refraction, and principles of ultrasonic testing is included for readers who are not experts in the field of vibroacoustics. Section 3, Measurements, gives a description of the equipment and materials used in the experiments. It is also intended to give insight to measurement setups and procedures. Stability issues and related techniques and procedures are also documented here. The section called "Results and discussion" presents the most important results in both time and frequency domain. The discussions of these results are placed in this same chapter.

2 Theory

2.1 Types of ultrasonic waves

Ultrasonic waves in isotropic materials are normally divided into three main groups; longitudinal, transversal and mixed type waves. The wave types are classified according to the direction of their particle vibration relative to the direction of propagation. The following is intended as a very brief general description of each wave type, and can be skipped by the reader who is experienced in the field of vibroacoustics.

2.1.1 Longitudinal waves

Longitudinal waves are longitudinal vibrations, i.e. vibrations parallel to the direction of propagation. They are sometimes referred to as compressional waves. Ultrasonic transducers normally generate longitudinal waves that in turn are converted into other wave types, e.g. in the interface between an angle-beam wedge and a test subject. Longitudinal waves is the fastest propagating wave type in steel, with a wave speed of approximately 5900 m/s [Olsen 1992].

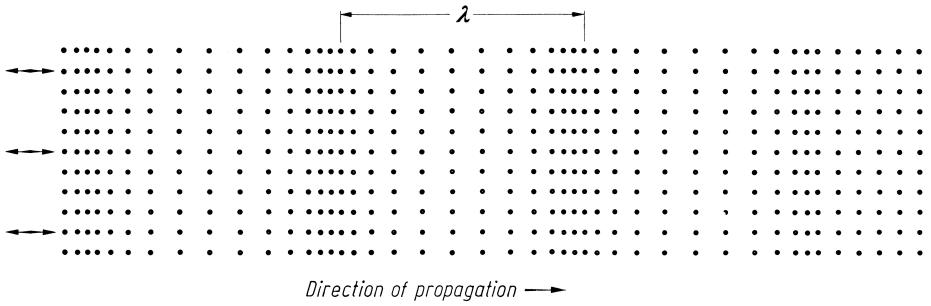

Figure 1: Longitudinal wave. Illustration from [Krautkrämer 1990].

2.1.2 Transversal waves

As the name indicates, transversal waves are vibrations perpendicular to the direction of propagation. These waves are often referred to as shear waves. In contrast to longitudinal waves, transversal waves are practically non-existent in fluids and gases. This is because transversal waves only propagate through materials where the particles are more firmly bound to one another than those in a liquid or gas. Transversal waves do not propagate through steel as fast as longitudinal waves but have roughly half the speed at around 3200 m/s.

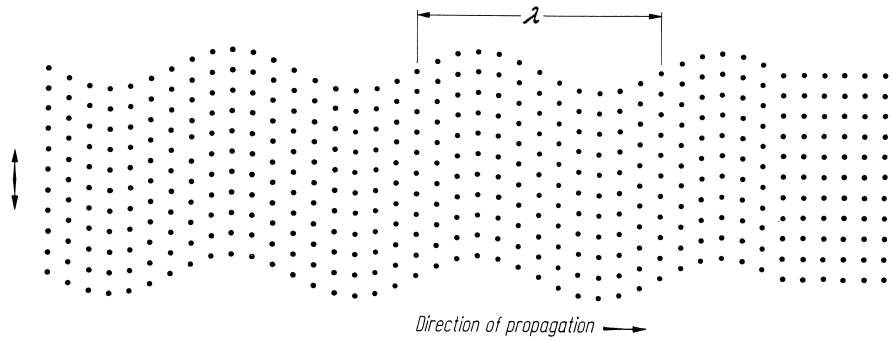

Figure 2: Transversal wave. Illustration from [Krautkrämer 1990].

2.1.3 Mixed type waves

Mixed type waves are waves that are a combination of longitudinal and transversal waves. Surface waves are a type of mixed type waves that propagate along a material boundary parallel to the direction of propagation. Rayleigh waves is the designation for one type of surface waves, and this type of waves is of particular interest for use in non-destructive testing. The particle movement in Rayleigh waves follows elliptic paths. Therefore these waves can neither be classified as purely longitudinal nor transversal. Waves that can only propagate along a boundary are often described as *guided waves*. In contrast to *free waves,*guided waves cannot propagate freely in an unbounded medium. Rayleigh waves can propagate over relatively long distances if the impedance difference between the two materials is very large. Rayleigh waves are slightly slower than shear waves in steel, with around 92 % of the speed. [Krautkrämer 1990] As indicated in Figure 3, the particles on the steel surface follow elliptic paths. According to [Krautkrämer 1990], Rayleigh waves will follow the surface contour as long as the radius of curvature is not too small compared to the wavelength. This is a particularly interesting property with respect to the usefulness of Rayleigh waves in ultrasonic testing of materials.

If a Rayleigh wave is to propagate along a surface without becoming distorted, the depth of the solid needs to be large compared to the wavelength. In the opposite case, this surface wave will degenerate into a type of plate wave called a Lamb wave. Since the experiments described in this document involve only the case of wave propagation in geometries that can be assumed to be large compared to the wavelengths, plate waves will not be discussed further here.

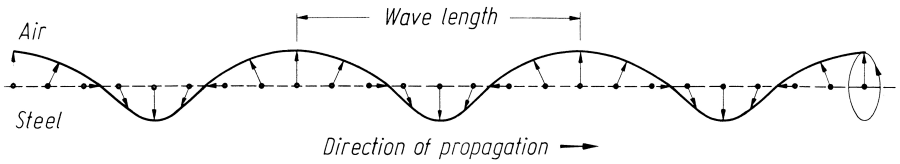

Figure 3: Rayleigh wave. Illustration from [Krautkrämer 1990].

2.2 Mode conversion and refraction at boundaries

When an incident wave strikes a plane interface to a different medium, it is well known that the energy will be divided between a reflected and a transmitted component. If the wave speed is not equal in the two materials, the transmitted wave will be refracted into the new material. The new direction is defined by the well-known Snell's law, equation (1), originally describing phenomena in optics. (c denotes wave velocity and α denotes the angles in medium 1 and 2.)

$$\frac{\sin \alpha_1}{\sin \alpha_2} = \frac{c_1}{c_2} \tag{1}$$

Snell's law applies to all types of plane wave propagation, including bulk mechanical waves transmitted from one medium to another. However, this relation between incident and transmitted waves is not sufficient to describe this situation. This is because a mechanical wave in a solid can be converted into a number of different wave types as it is transmitted into a different medium. This phenomenon is often referred to as *mode conversion* or *mode changing*.

Most of the measurements described in this thesis were carried out using so-called angle beam transducers and wedges (Figure 8). This equipment is based on the fact that waves can change modes as they pass through an interface between two different materials. The type of waves and direction in which they are transmitted is dependent on a number of different parameters such as the material properties, the coupling between the materials, the incident angle, the type of incident wave and its polarization if polarized. Figure 4 shows how an incident longitudinal wave in a plastic wedge can be converted to different wave types depending on the angle of incidence on the interface into steel. As the figure shows, the longitudinal waves are transmitted into the steel at angles smaller than the first critical angle of 27.6°. (The angle is referenced to the normal axis of the plane interface between the two media.) Except at this angle, the incident longitudinal waves also partly convert into transversal waves at all angles up to the second critical

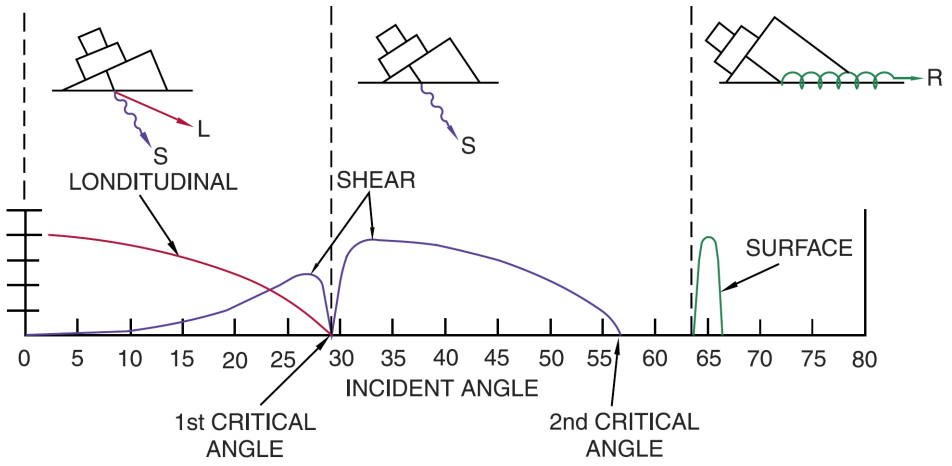

Figure 4: Relationship between the incident angle of a longitudinal wave, and the relative amplitudes of the refracted or mode converted longitudinal, shear, and surface waves that can be produced from a plastic wedge into steel. From [Olympus 2006].

angle of 57.8°. For larger angles there is only a surface wave transmitted in a small region around 65° incident angle.

2.3 Principles of ultrasonic testing of materials

2.3.1 Pulse-echo and pitch-catch

Ultrasonic testing (UT) is normally conducted in one of two different ways. Either it is a setup where the same transducer both transmits and receives the signal, or it is a setup with two transducers; one transmitter and one receiver. The former is called a pulse-echo (p-e) setup, while the latter is known as a pitch-catch (p-c) setup. The principles of the two setups are illustrated in Figure 5 copied from [Persson 1993]. Each method has advantages over the other, so the choice of method is largely dependent on the kind of object that needs to be tested, and the data required from the test. The p-e method is for example suitable for short range measurements of welds or for thickness gaging. The p-c method is sometimes used for detection of small defects that are not large enough to give clear reflections with the p-e method [Cartz 1995]. If it is desirable to cover a larger area in each measurement, the pitch-catch method is often used, for example in tomography setups, (example: [Hinders 2002]).

When using the p-e method for detection of material flaws, the most common strategy is quite simply to look for echoes with different arrival times than

those expected from the material boundaries. In thickness measurements using p-e the thickness is calculated by measuring the time it takes the wave to return from the material boundary. This is often referred to as a *time-of-flight* measurement. When using the p-c method it is more common to measure the amplitude or pulse shape deformation for flaw detection. This is the method that was used in all experiments that are described in this thesis.

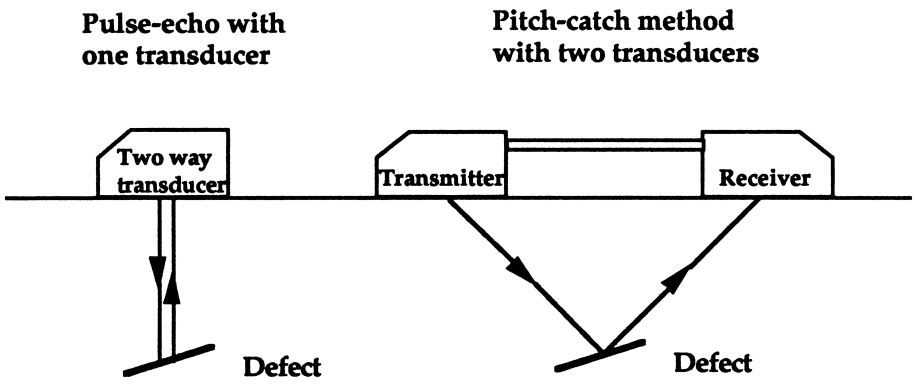

Figure 5: Principle drawing of the two most common UT setups; pulse-echo (left) and pitch-catch (right). From [Persson 1993].

2.3.2 Wavelength, sensitivity and range

In ultrasonic testing, wavelength rather than frequency (though closely related) is the interesting parameter with regards to limitations on sensitivity and range. Short wavelengths enable detection of smaller cracks and other flaws, whereas longer wavelengths give less undesired scattering and makes testing over longer distances possible. For this reason, the choice of frequency range has to fit the properties of the test subject. For example cast-iron has such a coarse material structure that relatively long wavelengths are needed in order to limit the unwanted scattering of the signal as it propagates through undamaged material. On the other hand the wavelengths must be short enough so that there is sufficient interference with the defects to make them detectable.

Table 1: Key parameters for vibrational waves in steel, [Krautkrämer 1990]

Wave type	Wave speed in steel [m/s]	Wavelength at 1 MHz [mm]
Longitudinal	5960	6.0
Shear	3235	3.2
Rayleigh	2975	3.0

For the measurement setup to be applicable for the SmartPipe project, there are limitations to the physical size of the transducers. Since the transducers are meant to be integrated in the encapsulation of pipes in inaccessible locations, it is a great advantage if the signals are simple enough to be processed locally. All of this points toward the choice of a high-frequency measurement system.

3 Measurements

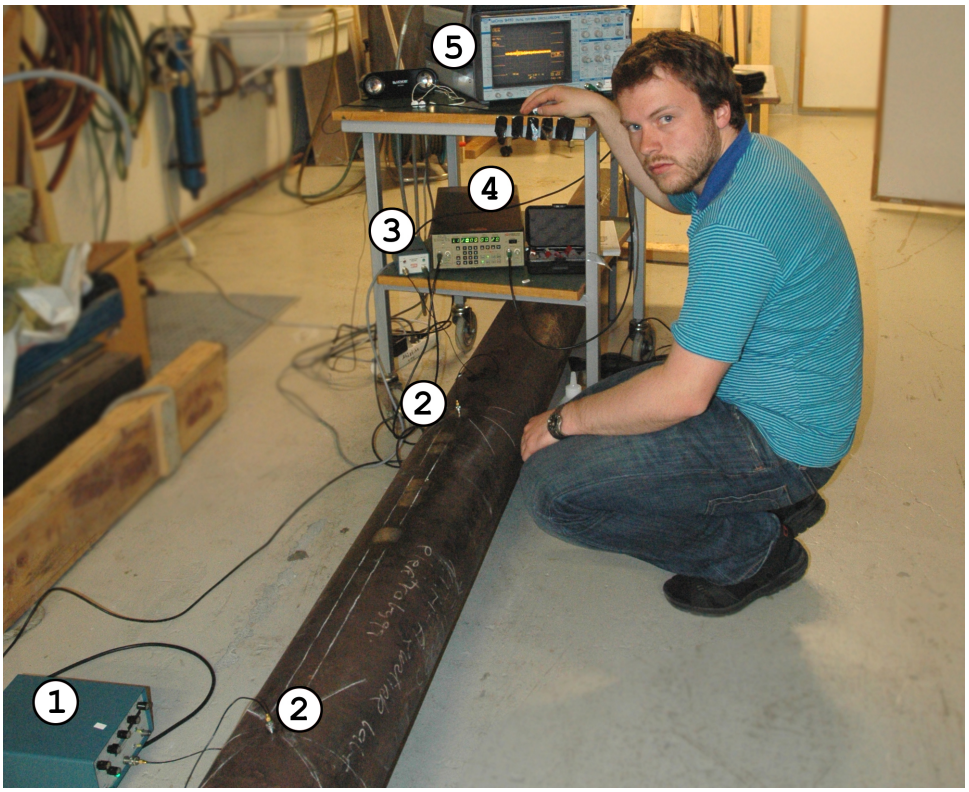

Figure 6: Overview of measurement setup. 1: pulser, 2: transducers (here without wedges), 3: preamplifier, 4: high-pass filter, 5: oscilloscope

All measurement results presented in this thesis were performed with the equipment depicted in Figure 6, represented schematically in Figure 7. This section is a description of the different equipment and materials used. It also describes the procedures and techniques that were used in order to attain the results presented in section 4.

3.1 Measurement objectives and overview

From the very start, the idea of the measurements was to learn if ultrasonic waves could be created and detected on a steel pipe with a relatively simple measurement setup. The second step would then be to introduce some kind of discontinuity on a the steel pipe and learn how this would affect the signal at the receiving end. This is also what was actually carried out in the lab.

As expected from the beginning, measurement repeatability would be one of the main challenges associated with the experimental work. Experiment-

ing with different types and amounts of couplant, and performing repeated measurements to check the measurement consistency was actually the most time-consuming part of the project. After achieving a satisfactory degree of repeatability, the pipe was damaged by sawing a crack between the transducers. Measurements were performed during the process of sawing, so that the dependency between the crack depth and signal degradation could be documented.

3.2 Measurement setup

The measurement setup (illustrated schematically in Figure 7) is quite simple. A unit called a *pulser* produces an electrical signal that drives a transducer with a piezoelectric element. The transducer is mounted on a steel pipe using a viscous couplant. The vibrations propagate in the pipe wall and are picked up by a similar transducer which in turn converts them into electrical signals. These signals are amplified and filtered using a preamplifier and an adjustable high-pass filter with 20 dB input gain, before they are averaged, recorded and displayed by the oscilloscope. Due to the different signal-to-noise ratios with different types of wedges, different numbers of averages were also used. With the 90°, 70° and 60° wedges, 250 averages were used. (Exception: When measuring over a longer distance, 2500 averages were used.) With the 45° and 30° wedges, as well as with the transducers directly on the pipe, the number of averages was increased to 1000.

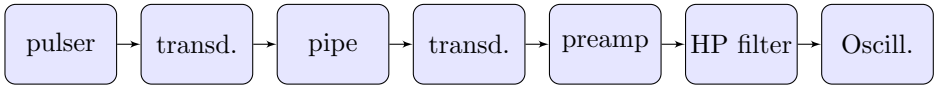

Figure 7: Schematic representation of measurement setup

3.2.1 The steel pipe

All measurements were performed on a 203.2 mm (8 inches) inner diameter steel pipe with a wall thickness of 8.5 mm (1/3 inch). The length of the pipe was approximately 4.77 m, thus potentially introducing end reflections after a certain amount of time depending on the placement of the transducers and the wave type. In almost all measurements the transducers were placed in a tandem configuration with 1.00 m axial separation. With the transducers placed like this, the longitudinal waves reflected from the pipe ends arrive after a minimum of around 0.8 ms.

The pipe had previously been used for other experiments and had several small scratches, some of these more severe with depths of around 1 mm. The pipe did also have remains of a few welds on the outer surface, but

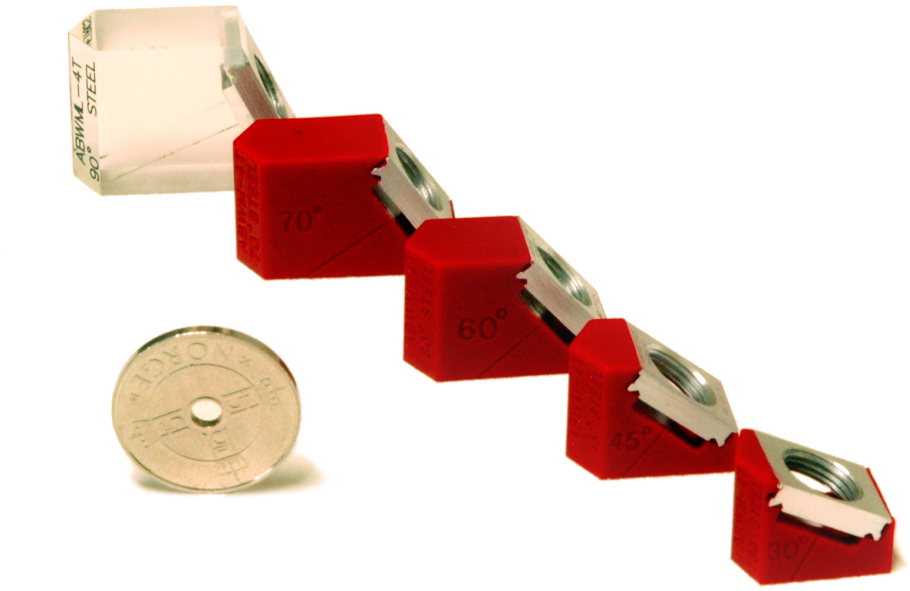

Figure 8: Wedges for introduction of shear waves at various angles into steel. From the left: 90, 70, 60, 45 and 30 degrees. Angles measured from the normal axis of the plane of the interface between wedges and steel. (The coin is a Norwegian krone serving as a size reference.)

except from one weld, these had been removed and the surface smoothed out. The heat-affected zones (HAZ) could of course not be removed, so these areas were also avoided during measurements. The surface of the pipe was generally slightly uneven with shallow grooves. Suitable equipment for measurement of surface unevenness was not available during the project, so this property could not be properly quantified. From visual inspection, the depth of the general unevenness of the pipe surface was estimated to be in the range of around 0.1 mm [1]. The unevenness seemed to origin from the pipe production process.

Because of the unevenness and existing damage on the pipe, very different results were obtained when measuring in different positions on the pipe surface. Such an unfavourable situation makes absolute measurements impossible, but since the project was at an introductory stage it was decided

[1]The unevenness was examined by holding a metal ruler across the grooves, but they were too shallow to be measured this way. The estimate of 0.1 mm is very rough, and is only based on a comparison between the grooves and the 0.25 mm deep crack produced with a hacksaw.

that relative measurements was an acceptable alternative.

Offshore sub sea pipelines are typically wrapped in protective plastic coatings of various thicknesses. Different fluids and gases are often transported simultaneously in the same pipe. Pipes used like this are often referred to as multi-phase pipes. The plastic wrapped type of pipe was not available to the project, and for rather obvious practical reasons a multi-phase flow could not be recreated in the lab. However, we can assume the acoustic impedance of the plastic coating to be very small compared to the impedance of steel, thus making the observations of a steel pipe surrounded by air acceptable as an indication of the behaviour of a plastic wrapped pipe.

3.2.2 Transducers and wedges

At the beginning of the work on this thesis, contact type transducers were not available. Because of an unfortunate series of events, suitable transducers were not acquired until relatively late in the project. To make the most of the time while waiting for the contact transducers to arrive, a pair of 1 MHz immersion type transducers were used for initial testing of the measurement setup. These transducers are produced by Panametrics, are designated C302-SU, and have a nominal element size of 25.4 mm (1.00 inch) diameter. See appendix II for data sheet.

This report has its emphasis on the measurements made with a set of so-called angle beam transducers with a center frequency of 5 MHz. These transducers are also produced by Panametrics. They are designated V543-SM and have a nominal element diameter of 6 mm (0.25 inches). These transducers are a single element type used with various wedges, see Figure 8. The red wedges in Figure 8 are specially designed to create refracted shear waves at various angles in steel. The transparent wedge (referred to as a 90° wedge in the following) is designed to introduce surface waves in steel. Most of the measurements were carried out using this kind of wedges. All measurements (with or without wedges) were performed with rubber bands holding the transducers and wedges in place. A 5 MHz transducers mounted on the pipe with a 90° wedge is shown in Figure 9. For data sheet, see appendix II.

3.2.3 Pulser and preamplifier

The pulser is the unit that supplies the transmitting transducer with the necessary signal to vibrate the way that is desired. The Panemetrics pulser/receiver model 5052PR was used as pulser on this project. This pulser has very few, yet important variable settings that should be understood by the operator for best possible results. Energy is one of these settings. This variable ad-

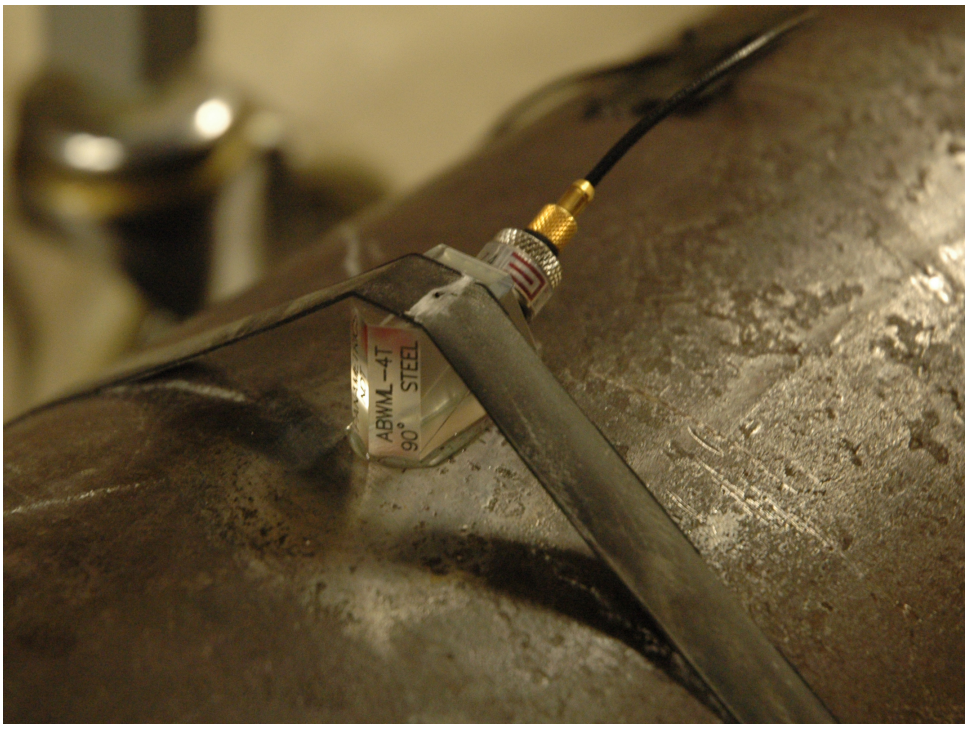

Figure 9: Transducer mounted on steel pipe with 90° wedge, ultrasound gel and rubber band. Note that in this picture, the tool for applying gel has not been used and gel is therefore visible in front of the wedge.

justs the signal energy, and according to the user manual, it should be kept at one of the lower settings when signals with higher frequency-content than 5 MHz are desired. However, it should be kept in mind that high-frequency signals in steel are generally damped more easily than low-frequency signals so keeping the signal energies at a certain level is desirable with respect to signal-noise ratios. A second setting that also is crucial for the pulse shape and amplitude is the setting for signal damping. This variable controls how quickly the transducer oscillation is damped by adjusting the resistive load presented to the transducer. A high damping should be used to obtain short bursts with clean damped pulses, but a high damping dramatically reduces the signal energy and this should be kept in mind when setting this variable

During the measurements for this project both the energy setting and the setting for damping were set to their maximum values. As the results presented in section 4 indicate, the signal-to-noise ratios were very good for the measurements with wedges with higher angles of incidence, and much lower for the 30° wedge and measurements without wedges. The low signal-to-noise ratios in these measurements could perhaps have been improved by

slightly reducing the damping.

The preamplifier is also a Panametrics unit. This unit has no user-adjustable variables. The signal conditioning carried out by the preamplifier is a pure amplification. It does not filter away any of the noise. However, the amplified signal is more noise resistant as it passes through the remaining units of the measurement chain, and it was found that it improved the signal-to-noise ratio.

3.3 Initial measurements – coupling and stability

Before introducing any discontinuities on the steel pipe, initial measurements were performed in order to develop measurement techniques that would provide the necessary degree of repeatability. Mainly results from measurements with 5 MHz transducers are discussed in this thesis, but information regarding coupling and stability in measurements with 1 MHz transducers is also included since it could be of use in further laboratory work on the SmartPipe project. Mechanical coupling between the transducers, wedges and the steel pipe turned out to be a one of the main challenges involved with the measurements.

3.3.1 1 MHz transducers

Since the first measurements were performed with 1 MHz immersion type transducers with diameters of 30 mm, mounted directly on the pipe, the curvature of the pipe resulted in a gap on each side of the transducers. Without any couplant between the transducers and the pipe, hardly any energy at all was transferred into the pipe. Water, mayonnaise and ultrasound gel were tested as couplants between the transducers and steel pipe. Ultrasound gel was found to be easier to work with than water because of the higher viscosity. Mayonnaise has much of the same qualities as the ultrasound gel, except from the favourable property that the gel is practically odourless even when left to dry. All of these couplants increased the amount of transferred energy enough to provide usable signal-to-noise ratios, but the signal stability was still not good. The main reason for this was probably the varying amounts of couplant and the relatively wide gaps between the large flat contact surfaces of the transducers, and the curvature of the pipe. In order to improve the stability, circular adapters were produced in lexan. Since these were curved on the side facing the pipe and flat on the transducer side, the required amount of couplant was reduced to two very thin layers. Ultrasound gel was then acquired and used instead of mayonnaise.

The measurement stability was much better when using the adapters and reduced amounts of couplant. Figure 10 shows an example of a stability

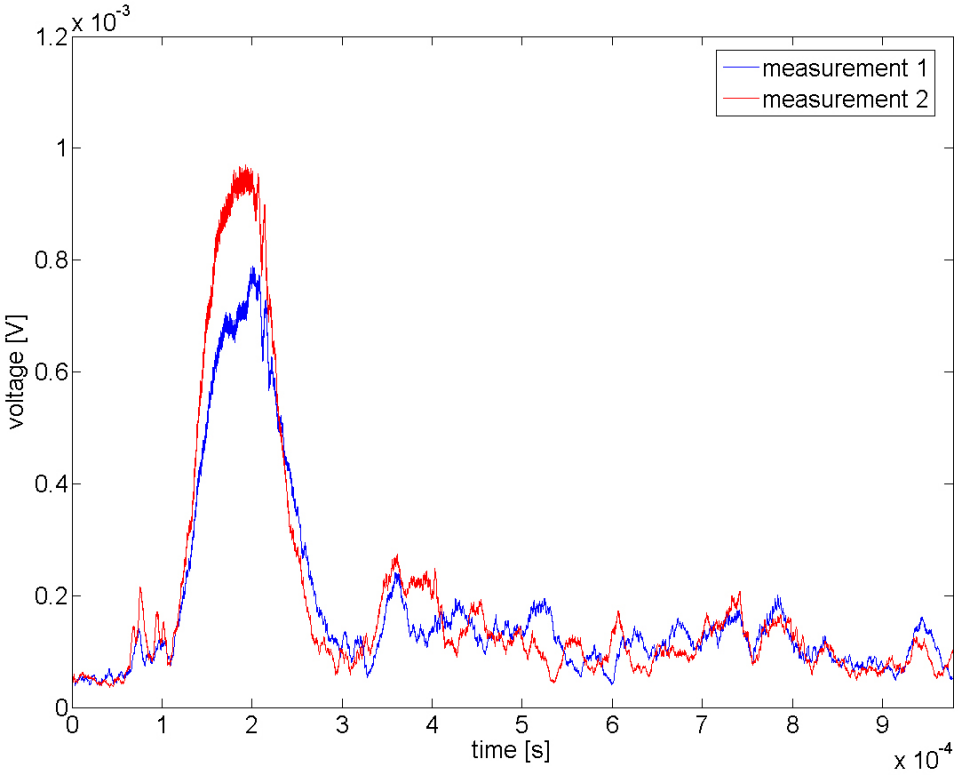

Figure 10: Example of results from stability test with 1 MHz transducers with lexan adapters and gel for coupling. 0.23 m distance between transducers. Note that these measurements were recorded without the 20 dB gain of the HP-filter, used in all other measurements.

test with the 1 MHz transducers, lexan adapters and ultrasound gel. The plotted graphs are 50 µs moving time averages of the absolute values of the recorded signals. The graph with the legend ”measurement 2” is simply an attempt to recreate the measurement shown with legend ”measurement 1”, as exactly as possible. As this figure shows, the stability could be adequate for some measurements, but not good enough to see small changes in the amplitude e.g. caused by very small discontinuities on the pipe. As we can see by comparing this figure with for example that from measurements with 90°, 70° and 60° wedges (Figure 16), the energy of the pulse from the 1 MHz transducers is not as concentrated in the main peak. In contrary to the results from measurements with wedges, the results with 1 MHz transducers have long tails of relatively high amplitudes following the main peak. The somewhat more complex pulse shape of the 1 MHz transducers is probably due to multi mode transmission, i.e. multiple wave types are transmitted simultaneously. As we will see in the results presented in the following, the same phenomenon appears also when using 5 MHz transducers directly on

the pipe or with the 30° and 45° wedges). The 5 MHz transducers, especially with the 90°, 70° and 60° wedges, were generally much simpler to work with than the 1 MHz transducers (used without wedges), because of their superior measurement stability and few sharp peaks in the signal envelopes. This is the reason why the section with results and discussion section will focus on the 5 MHz transducers only.

3.3.2 5 MHz transducers and wedges

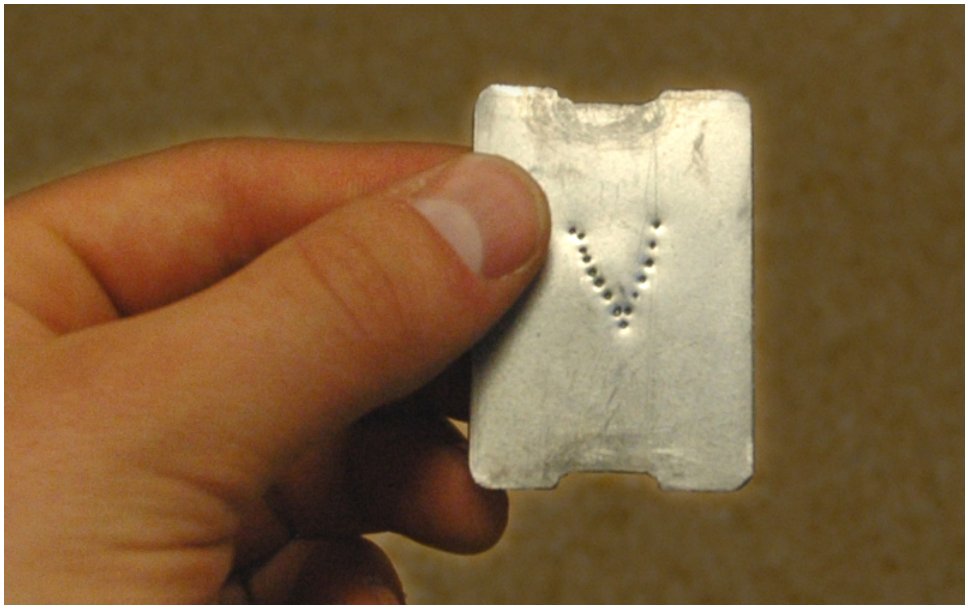

Figure 11: Simple tool used to apply consistent amounts of gel to wedges. (The widths of the profiles on each side are slightly different in order to fit different wedges. The symbol < is just there to indicate which profile is the widest.)

Mounting the 5 MHz transducers and wedges directly on the steel pipe with no couplant was also tested and again clearly showed that very little energy was transferred into the steel. Since the ultrasound gel provides sufficient mechanical coupling to steel and satisfactory signal-to-noise ratios, it was used in all of the measurements presented in the following. However, simple measurement repeatability tests revealed a large measurement-to-measurement variation in amplitudes. It was suspected that the slightly varying amount of ultrasound gel that was applied manually between each measurement could be the cause of the variation. The suspicion was confirmed after some further testing with different amounts of gel. In order to get an increased repeatability, a very simple tool was made so that the same amount of gel could be applied to the wedges before every measurement. The tool was not made to

leave any specific amount, but the layer of gel had a thickness on the order of 1 mm. This increased the measurement stability further, and was used in all measurements from which there are results presented in this document. Because of the function of this tool, hardly any gel was applied to the tips of the wedges. When the wedges were pressed against the pipe with the tips first, the area in front of the wedges was kept almost completely clean from gel. As mentioned in the theory section, it is very important for the propagation of surface waves that the area immediately in front of the wedge is kept dry.

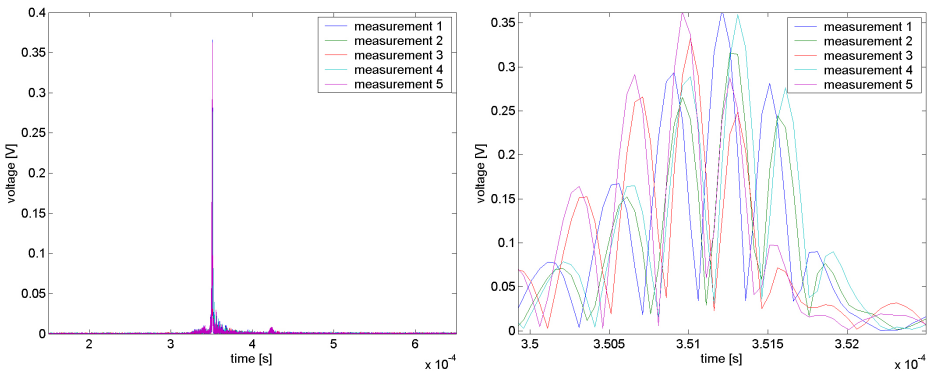

Figure 12: Result from stability test with 90° wedges and gel applied with tool. The plot to the right is a zoomed selection showing the highest peaks of the plot to the left.

3.4 Measurements on damaged pipe

After a satisfactory degree of repeatability was attained, it was possible to carry out measurements to document the influence that a crack in the pipe surface would have on the signal propagation. A distance of 1.00 m was measured and marked on the pipe. A distance of 1.00 m between the transducers means that with a maximum propagation speed of 5960 m/s (speed of longitudinal waves in steel), the earliest possible arrival of propagated signals will be after a time of approximately 168 µs. Since the transducers were placed close to the middle of the pipe, the minimum distance from the sending transducer to one of the pipe ends and back to the receiving transducer was approximately the same as the length of the pipe, namely around 4.5 m. This gives an earliest possible arrival of end reflections after approximately 755 µs. Since the measurements were not exactly at the middle of the pipe the results were assumed to be free from end reflections until at least 650 µs. For these reasons most of the results plotted in the time-domain are presented with a time-axis stretching from 150 µs to 650 µs.

As mentioned in section 3.1, the strategy was to perform measurements during the process of sawing into the pipe. The initial plan was to use a single pair of wedges and do measurements for every 0.25 mm increase in the depth of the crack. The measurement stability would be maximized by leaving the two transducers untouched throughout the whole process of sawing and measuring. Unfortunately, the ultrasound gel began to dry out before the planned 21 measurements and 20 turns of sawing could be completed. The change in the properties of the gel meant that the results from these measurements had to be discarded. Since leaving the two wedges untouched during the procedure could not be done using ultrasound gel, it was decided that it would be best to apply new gel for each measurement. Since this meant that the transducers would be removed from the pipe between measurements, it also meant that measurements could be carried out with multiple wedge types. It was decided that measurements with the 90° wedges would again be carried out for every 0.25 mm increase in the depth of the crack. The 70° and 60° wedges would be used to measure the progress for every 0.5 mm. The wedges with lower refracted angles (45° and 30°) as well as measurements with the transducer directly on the pipe were limited to before/after-measurements. The restricted number of measurements was chosen due to the limited time available for both measurements and analysis.

4 Results and discussion

The results from the measurements are mostly given as graphs showing the absolute value of the time-signal from the receiving transducer. Even though they represent the vibrational amplitude that is picked up by the receiving transducer, the vertical axes of these plots are simply labeled "voltage [V]". Since the measurements are all relative to one another, calibrating and scaling the units was considered unnecessary, and therefore not prioritized. For this reason, energy considerations will not be in any standard unit, but in dB relative to 1 V^2s. Frequency spectra are RMS-squared, and have the unit [dB rel. 1 V^2] on the vertical axis. Again, the important thing for the understanding of the following results is not the numbers and their units, but the comparisons of measurements.

As explained in section 3.2, averaging was employed in order to suppress uncorrelated noise. Most measurements are based on 250 averages, but with some setups it was not even possible to see the bursts on the oscilloscope without averaging, and as much as 1000-2500 averages were used in order to get a good signal-to-noise ratio.

4.1 Time domain

The analysis of the time domain results is heavily based on the arrival times of the various peaks in the signal envelopes. The determination of the arrival times was done manually and a somewhat loosely defined criterion was chosen due to the varying shapes of the signal envelopes. Generally the start of the leading edges of the envelope peaks were sought and used to define the arrival time of a burst. If the signal analysis is to be carried out automatically there are several ways to define this criterion, but since all analysis was done manually this was not necessary.

The time domain results are also averaged with a 2.5 µs moving window average of the absolute value of the received signals. The moving average was used in order to smooth out the graphs for legibility and to make comparisons of different measurements simpler.

4.1.1 Rayleigh waves

As indicated in the plot to the left in Figure 13, the 90° wedges (for excitation of Rayleigh waves) give a very sharp and pronounced peak around 350 µs. When zooming in on the same plot, we see that the peak is not really a single peak, but rather a short burst of oscillations. The wave speed is calculated to be approximately 2857 m/s, based on an arrival time of 350 µs and a distance of 1.00 m. This is a slightly lower speed than the theoretical

speed of 2975 m/s for Rayleigh waves. However, if we subtract the theoretical time it takes for the vibrations to propagate through the wedges in the form of longitudinal waves (estimating the longitudinal wave speed very roughly as 2700 m/s), we end up with a wave speed of 2979 m/s for the Rayleigh waves on the pipe. This means that the measured wave speed is as good as equal to the predicted wave speed for Rayleigh waves. Therefore the arrival time of the burst does support the assumption that the received waves are transferred in the form of Rayleigh waves.

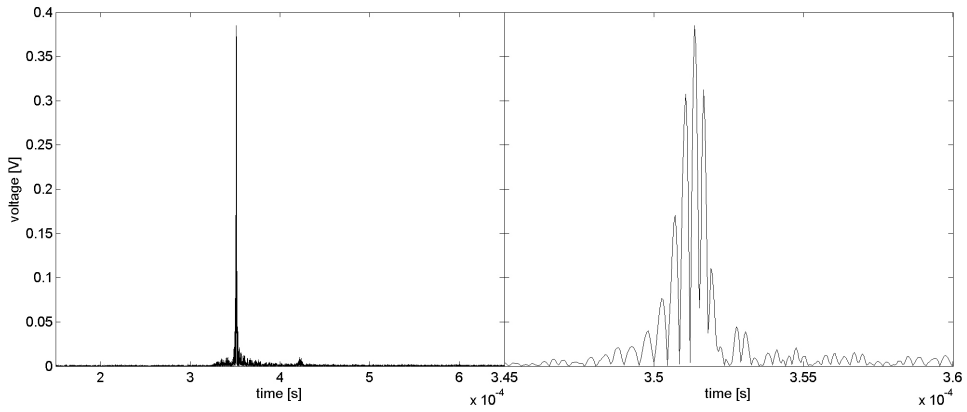

Figure 13: Absolute value of received pulse with 90° wedges for excitation of surface waves. Left: complete recorded data. Right: Zoomed selection from same data. (Distance between wedges: 1.00 m)

As Figure 16 shows, the main bursts have almost similar arrival times also with some of the different sets of wedges. This could be an indication that the main bursts are actually formed by Rayleigh waves even when using wedges for refracting shear waves into steel at 70°, 60° and 45°. An alternative explanation is that the shear waves follow zigzag paths and therefore their arrival times will be delayed corresponding to a reduction of the wave speeds by a factor $\sin(\theta)$, where θ is the angle between the refracted wave and the normal to the pipe surface. This explanation matches the recorded arrival times roughly for the 70° and 60° wedges, but the arrival time with the 45° wedges contradicts this theory.

In contrary to the theory of zigzag paths, the arrival times of the main bursts match the theoretical arrival times of Rayleigh waves very well, especially if we take into account the different sizes of the various wedges. The wedges with larger angles of incidence (e.g. 90° and 70° wedges), are physically bigger and therefore introduce longer delays due to the extension they introduce to the path lengths. Table 2 shows the actual arrival times for

each set of wedges, as well as the corrected arrival times and wave speeds. The corrected values take into account the calculated time it takes for the vibrations to propagate through the wedges. Figure 14 shows the wedges used. The straight lines marked on the sides of the transducers indicate the angles of incidence of the longitudinal waves. The numbers indicate the angle at which the shear waves are refracted into steel. (As mentioned in section 3.2.2, the transparent wedges labeled 90° are designed to create a Rayleigh wave.) The mean of the corrected speeds is 2961 m/s. That is only about 0.6% lower than the theoretical speed. Since the standard deviation of these four values also is as low as 15.3 m/s, this is indeed an indication that the strongest signal bursts in measurements with 90°, 70°, 60° and 45° wedges, could all be formed by Rayleigh waves.

If this is actually the case, the acquired measurement data is not sufficient to find out why Rayleigh waves rather than shear waves appear to be picked up by the receiver. It is possible that the shear waves *are* refracted into the steel, but that these waves are converted into Rayleigh waves as soon as they run into the outer surface of the pipe. Excess ultrasound gel surrounding the bases of the wedges, or bad coupling between the flat-based wedges and the curved pipe surface, could be plausible explanations for why Rayleigh waves rather than shear waves seem to be picked up by the receiver.

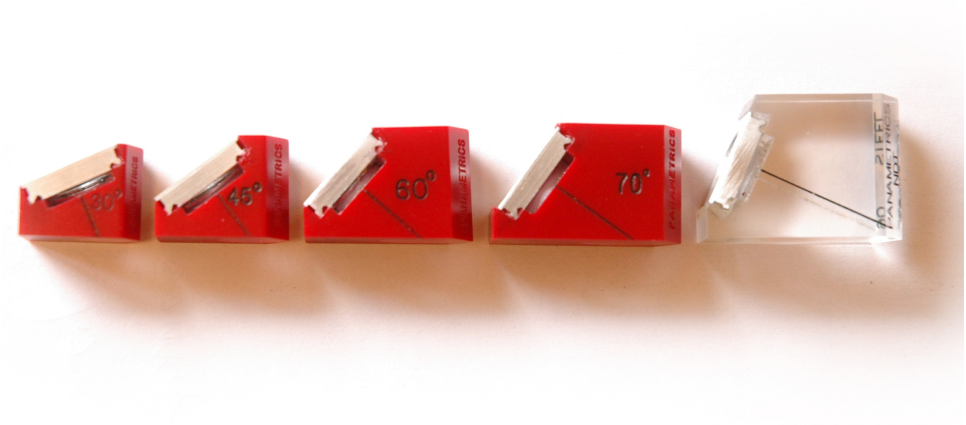

Figure 14: Sideview of wedges. Direction of incident wave indicated with black lines. Numbers indicate angle of refracted shear waves.

Regarding the corrected wave speeds in Table 2, it should be noted that the corrections are based on the estimated path lengths in the wedges. These measurements were not very accurate, since the paths are not uniquely defined by the lines marked on the sides of the wedges. The shortest paths are shorter than these lines and were determined by qualified guessing. For every

mm error in the measurements of the path lengths through a wedge, the corresponding corrected wave speed is changed by approximately 6 m/s. The assumed longitudinal wave speed of 2700 m/s in the wedges is based on the longitudinal wave speed in perspex (2730 m/s) according to [Olympus 2006]. The actual wave speed is not known precisely, since it was not measured, and is not provided by Panametrics. As already mentioned, the actual arrival times were determined by manually identifying the beginning of the start of the envelope peaks. All of these potential sources of error could explain the slight difference between predicted and measured Rayleigh wave arrival times and wave speeds.

There is also a small burst appearing after around 420 µs in the leftmost plot in Figure 13. This peak appears too late to be formed by any type of wave propagating along the direct path between the transducers. The phenomenon will be discussed further in section 4.1.2 – Results from measurements with damaged pipe.

Table 2: Measured and corrected wave speeds and arrival times for some wedges

wedge type	t_{actual} [µs]	$t_{corrected}$ [µs]	$c_{corrected}$ [m/s]
90°	349	336	2979
70°	347	340	2945
60°	345	339	2949
45°	342	338	2956

4.1.2 Results from measurements with damaged pipe

As explained in section 3.1, the pipe was intentionally damaged by cutting it with a hacksaw. The cut was made tangentially, close to the middle of the pipe. Measurements with 90° wedges were carried out for every 0.25 mm increase in the depth of the crack produced by the saw. To limit the amount of measurements, the measurements were only carried out for every 0.5 mm using the 70° and 60° wedges. These measurements revealed that the amplitude of the burst is decreasing for every increase in the depth of the cut into the pipe surface, and the decrease is significant even for the first 0.25 mm with the 90° wedges. The 70° and 60° wedges do not seem to be that sensitive to a shallow cut, but also with these wedges, the amplitudes seem to decrease even with as little as 0.5 mm depth of the crack.

Figure 15 shows the received bursts when using the 90° wedges for introduction of Rayleigh waves. One graph is shown for every millimeter increase in the depth of the cut in the pipe surface. As mentioned, measurements were performed for every 0.25 mm, but to keep the plot clear and legible, only a

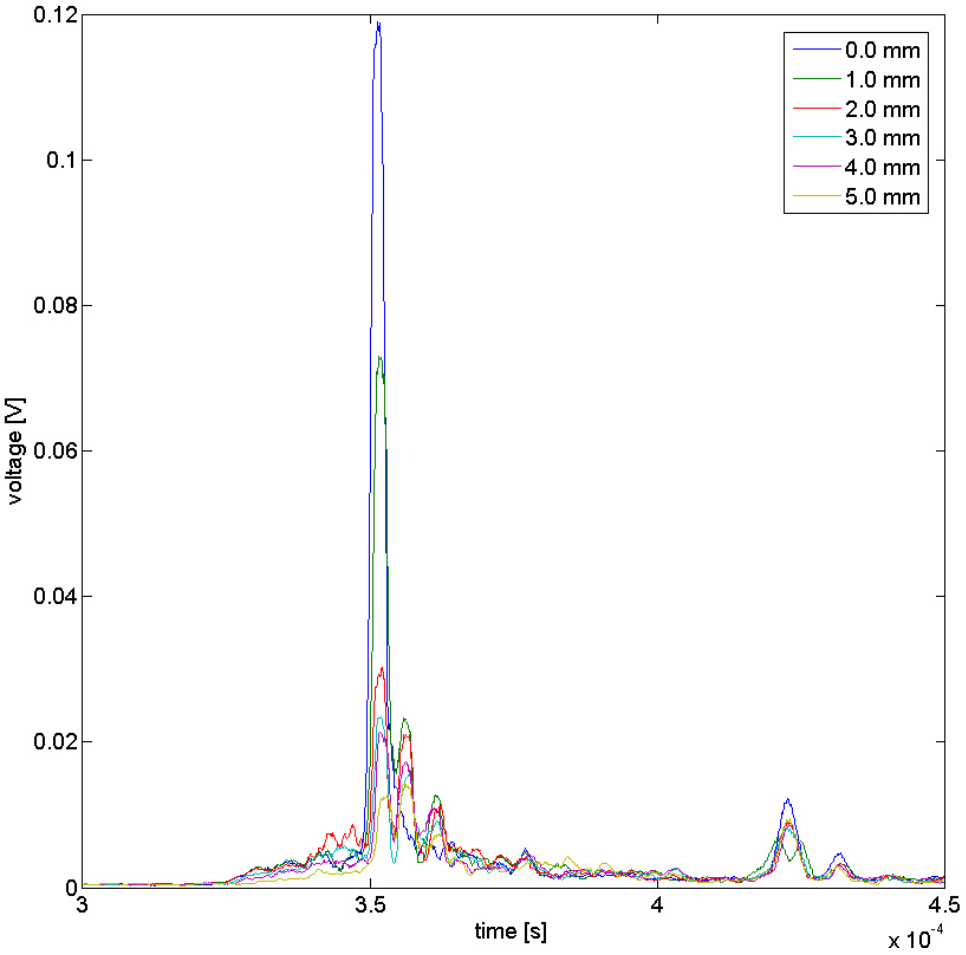

Figure 15: The effect of increasing cut depths in the pipe surface. Moving time average of absolute value. 2.5 µs window length. 90° wedges. 1.00 m distance.

selection of data is presented. The plot only shows the data from 300 µs to 450 µs since signals outside this window are much weaker, and seem to be some form of noise. The amplitude of the main peak in this plot, seems to drop in a quite predictable manner as the size of the damage increases. The only unpredictable change in the envelope shape happens between the measurement of the unharmed pipe and the 1.00 mm deep cut. The two peaks that appear right after the main peak in the envelope, are almost completely absent before the pipe is damaged. After the cut is introduced between the transducers, these peaks appear and then diminish as the depth of the cut is increased. This could be a very favourable property of Rayleigh waves and could be an indication of the possibility of high sensitivity to damage on the pipe surface.

The plotted graphs in Figure 16 show the recorded time signals with 90°, 70° and 60° wedges (absolute value, 2.5 μs moving window average,) before and after the introduction of the 5.0 mm deep cut into the pipe. Looking generally at these three plots, one may conclude that the results are very similar whether 90°, 70° or 60° wedges are used. The main burst in each plot has an arrival time that indicates that these bursts are all formed by Rayleigh waves.

The small burst after around 420 μs appearing in Figure 16 and also in the upper plot of Figure 17, can possibly be explained as Rayleigh waves travelling around the pipe once on its way to the receiver. The wave speed corresponding to this path and arrival time is approximately 3010 m/s (corrected for delay introduced by the wedges). As Figure 16 shows, this weak delayed burst appears to be unaffected by the damage inflicted on the pipe. This too supports the theory that it is formed by Rayleigh waves that travel once around the perimeter of the pipe on their way to the receiver. This is true for the setups with 90°, 70° and 60° wedges, but bursts with very similar arrival times appear also in the before/after plots in Figure 17 for both the 45° and 30° wedges. However, with these wedges, the late arriving bursts *do* seem to be affected by the damage on the pipe, thus contradicting the theory of Rayleigh waves travelling around the perimeter.

There is also another interesting feature of the envelope peak arriving after around 420 μs in Figure 16. This peak seems to be stronger when produced with 70° or 60° wedges than when 90° wedges are used. If waves are actually travelling around the perimeter of the pipe, the reason why the amplitudes are increased by the 70° and 60° wedges, could be found in the way that Rayleigh waves are created with these wedges. Possibly, the wedges *do* refract shear waves into steel (like they are designed to do), which are then converted to Rayleigh waves in the interaction with the pipe surface. A second possibility is that the way the flat-bottomed wedges are coupled to the curved pipe, could give some form of direct Rayleigh wave excitation. This direct excitation of Rayleigh waves could possibly be less directional than the direct refraction by the 90° wedges, and therefore enhancing waves that take other paths than the straight line between the transducers.

These phenomena and suggested explanations have not yet been investigated through further experiments, but if the surface waves actually travel around the perimeter, these waves could give very useful information about the general condition of the pipe.

In the results from measurements with 45° and 30° wedges and measurements with the transducers directly on the pipe, the received signals become increasingly complex. With the 45° transducers the main envelope peaks

still seem to appear at the same time as with the 90°, 70° and 60° wedges, but signals also start to arrive after only around 200 µs. This means that more energy is reaching the receiver in the form of longitudinal waves, and possibly also as shear waves. The multitude of peaks appearing in the plots with 45° and 30° wedges could be due to an equally large number of interactions between the refracted shear waves and the surface of the pipe, thus producing a nearly continuous arrival of Rayleigh waves due to mode conversion.

The plot with transducers directly on the pipe (lower plot in Figure 17) has an interesting peak arriving as late as after approximately 475 µs. A somewhat similar peak could possibly also be identified in the plot with 30° wedges. These bursts arrive too late to fit the theoretical arrival times for neither longitudinal, transversal nor Rayleigh waves taking the shortest path along a straight line between the transducers. However, it is possible that for example shear waves follow zigzag paths inside the pipe wall, and therefore arrive as late as the measured bursts do. With the limited data available, it is hard to classify and explain these peaks. A second possibility that fits this late arrival time is that the peak is formed by Rayleigh waves propagating twice around the perimeter of the pipe. However, this is a theory solely based on the arrival time and must therefore be considered as a poorly substantiated suggestion.

There are also some periodic peaks arriving extremely early in this plot. The peaks are in fact signal bursts dominated by a 2.5 MHz component. As discussed in section 3.4, the earliest theoretical time of arrival for longitudinal waves is around 170 µs. Since these bursts appear even earlier, there is reason to believe that they are not formed by vibrations picked up from the pipe, but are formed by electrical noise that is correlated with the signal, and therefore not possible to cancel even with the use of extensive averaging. This noise does not appear in any of the other plots, but it is very possible that the electric isolation that the plastic wedges provide between the transducer and the steel pipe is the reason for this. When the transducers are placed directly on the pipe, a ground loop is formed, thus increasing the sensitivity to electrical noise significantly.

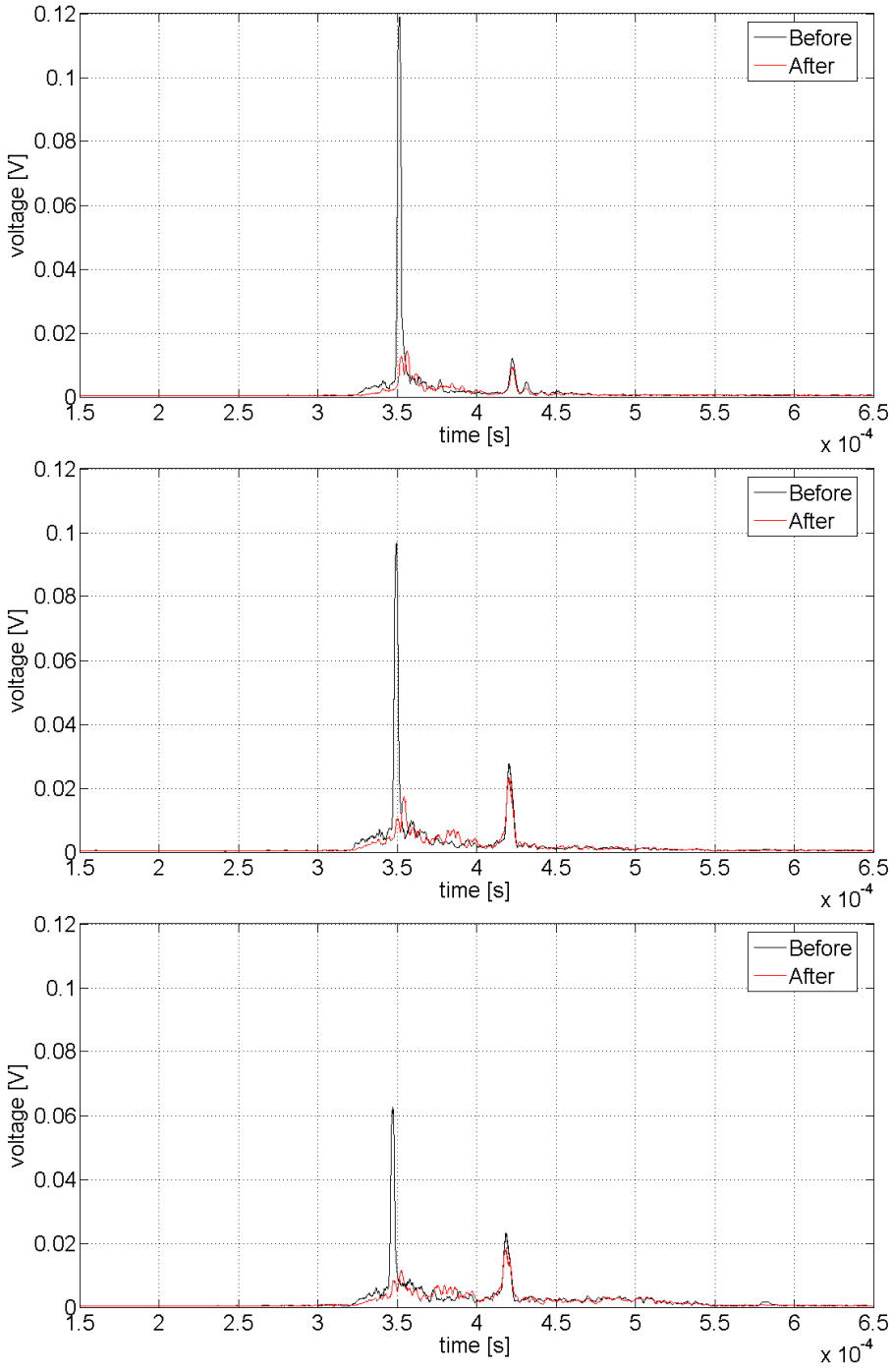

Figure 16: Moving time average of absolute value before/after introducing a 5.00 mm deep cut in the pipe surface. Top: 90° wedges. Center: 70° wedges. Bottom: 60° wedges. 2.5 µs window length. 1.00 m distance.

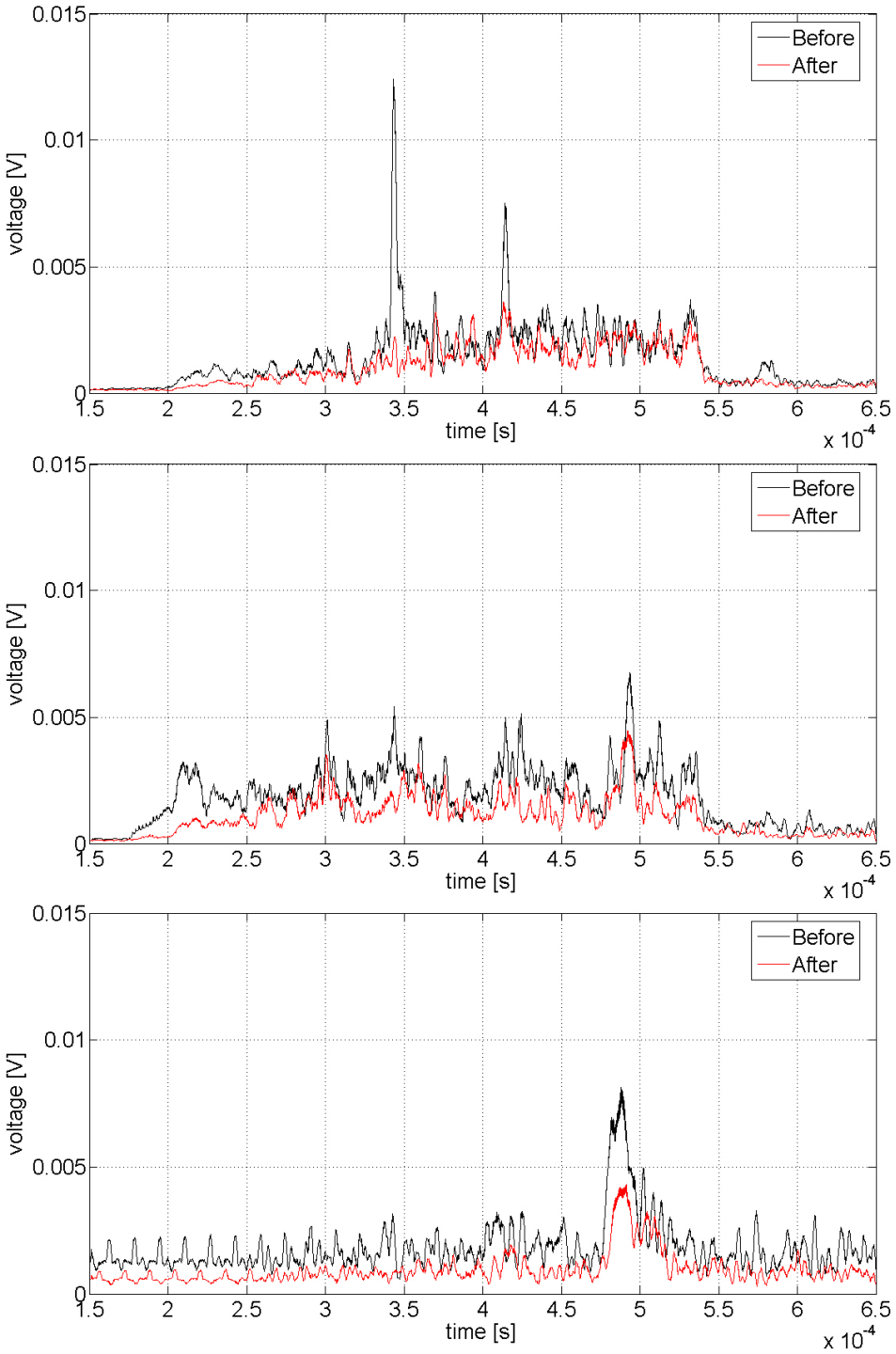

Figure 17: Moving time average of absolute value before/after introducing a 5.00 mm deep cut in the pipe surface. Top: 45° wedges. Center: 30° wedges. Bottom: No wedges. 1.00 m distance. (Note that vertical axis is different from Figure 16.)

4.1.3 Tests with 90° wedges and longer distance

Since the signal-to-noise ratios in measurements with 1.00 m distance between the 90° wedges were very good, it was assumed that measurements over longer distances would be possible. Because the available steel pipe did not measure more than 4.77 m in length, a 1.00 m separation of the wedges was considered a maximum in order to maintain sufficient separation between the direct signals and the end reflections. However, before/after measurements were also performed with as much as 4.38 m distance between the 90° wedges. Figure 18 shows the time-averaged absolute value of the received signals. The signal-to-noise ratios in these measurements were dramatically reduced, and extensive averaging was necessary in order to separate the signal bursts from the noise. In contrary to the 250 measurements that were averaged when using 1.00 m separation of the 90° wedges, 2500 measurements were averaged with the longer distance measurement in order to attain a similar signal-to-noise ratio.

As the plot shows, there are still rather distinct peaks appearing. However, instead of the two main peaks that appear when measuring over a distance of 1.00 m, 3-4 peaks appear. We cannot rule out the possibility of end reflections influencing these results, but the time separating the largest peaks is too long for one of them to be a reflection of the other. There is also reason to believe that the transducer does not pick up the end reflections very well, since they come from the "wrong" side of the wedge. If they are at all refracted into the wedge, they are probably still not picked up very efficiently by the transducer that is angled toward the other end of the wedge.

If we again resort to the arrival times when trying to classify the wave types involved, the predicted arrival time (assuming a longitudinal wave speed of 2700 m/s in the wedges, and 2975 m/s as Rayleigh waves in steel,) is calculated to 1.487 ms. This time is indicated by the leftmost flag in the plot, and fits well with the arrival of the first peak. Interestingly, the first peak remains almost unchanged after the damage is introduced to the pipe. The second and highest peak is actually higher when the pipe is damaged than when the pipe is unharmed. This is the only measurement where one burst in the pulse train is clearly stronger after introducing the damage, and is therefore hard to explain.

The three flags in Figure 18 indicate the theoretical arrival times of Rayleigh waves following the direct path, the path that goes around the perimeter once, and the path that goes twice around the perimeter. These three arrival times match three of the measured peaks strikingly well, but due to the somewhat strange amplitude changes, there is still doubt if the peaks are shaped by waves travelling around the pipe perimeter or not. Not only

does the highest peak grow when introducing the damage, but according to this theory, the second largest peak (with the flag X: 0.001559) should not have decreased after damaging the pipe. If it was travelling around the perimeter once, it should have remained unchanged by the damage. If the wedges would have been glued to the pipe surface, the stability would probably have been improved enough to rule out the possibility of an error due to inconsistent coupling between the wedges and the pipe. Even if the results from the tests with longer distance between the transducers were rather inconclusive, the tests still showed that through extensive averaging, usable signal-to-noise ratios could be attained, also when measuring on several meters of pipe length.

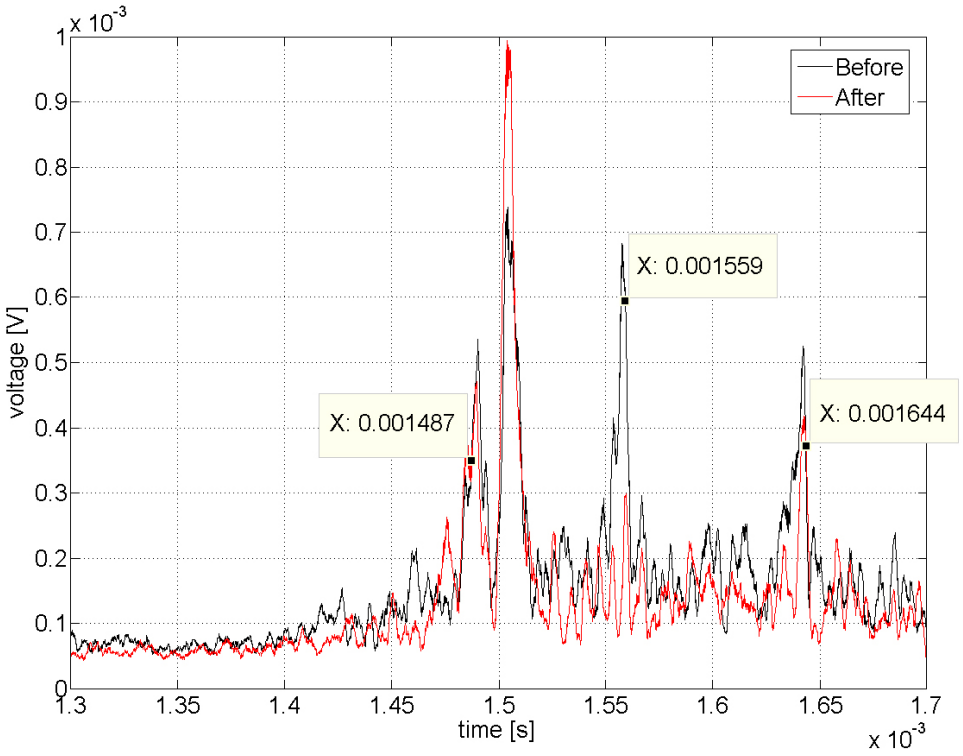

Figure 18: Moving time average of absolute value from measurement with 4.38 m distance between transducers, before/after introducing a 5.00 mm deep cut in the pipe surface.

4.2 Frequency domain

Quite broadband signal burst were produced by the pulser, and this is also reflected in the amplitude spectra of the recorded signals from the receiving transducer. Figures 19, 20 and 21 show the RMS-squared amplitude spectra of the received signals from measurements with 90° wedges, 30° wedges, and

without wedges respectively. Generally, the signal energy is centered around $1 - 1.5$ MHz. This is very far from the 5 MHz center frequency of the transducers (see Appendix II). The pulser settings could possibly account for part of this mismatch. The signal-to-noise ratios were sufficient to provide useful data, and if the transducers had actually been fed with a signal with a center frequency of 5 MHz, there might be a possibility that the signal-to-noise ratios could have been even better, and therefore good enough to measure over longer distances or with more lossy materials.

There is also a possibility that the relatively low frequency contents of the signals could have influenced the function of the wedges for introduction of shear waves in a way that enhanced the excitation of Rayleigh waves. However, Olympus/Panametrics refer to the wedges as "...Wedges for $1 - 5$ MHz" in their product catalog [Olympus 2006], making this theory seem somewhat unlikely.

The spectrum measured with 90° wedges (Figure 19) is very smooth with only a few local ripples of more than 5 dB before the pipe is damaged. After the introduction of the 5 mm crack on the surface, some of the ripples measure more than 10 dB peak to peak and the spectrum is generally more uneven. As Figure 19 also shows, the difference between spectra before and after damaging the pipe, is at its largest in the frequency range $0.8 - 3$ MHz. This corresponds to wavelengths in the range $1.0 - 3.7$ mm for Rayleigh waves. Since the crack is 5 mm deep, this fits well with the assumption that the discontinuity needs to be larger than the wavelength for detection to be possible. Since the crack is around 70 mm long, it can also be detected with wavelengths longer than the crack depth, but the influence on the propagating vibrations is not as strong. For frequencies above 3 MHz, the spectrum is almost unaffected by the damage on the pipe. The reason for this could simply be poor signal-to-noise ratios, but it could also be explained by the ability that Rayleigh waves have to follow curvatures that are relatively large compared to the wavelength. Since frequencies above 3 MHz have sub millimeter wavelengths, there is a chance that these frequency components are able to follow the curvature of the crack even if the edges are rather sharp.

Looking at Figure 20 we see that when the 30° wedges are used, the center frequency is slightly lower than with the 90° wedges. Also, the spectrum is more rugged, and is actually slightly smoother after the damage is introduced, –especially above the center frequency. The reason why these spectra are different from those in Figure 19 is probably that the vibrations are no longer as dominated by Rayleigh waves, but are a composite of shear waves and longitudinal waves. Since these wave types have different wave speeds and therefore also different wavelengths, there is for example not just one single transition in the ratio between wavelength and the depth of the crack.

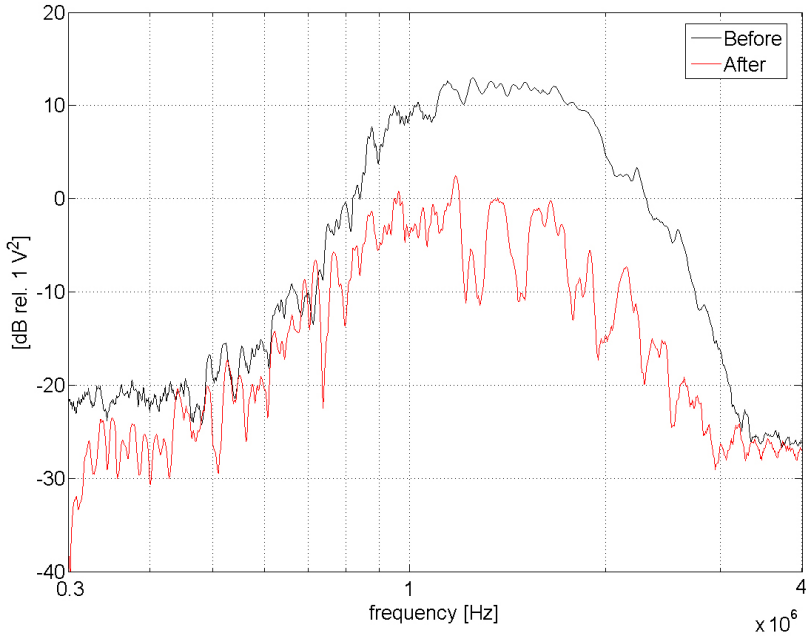

Figure 19: RMS-squared power density spectrum before/after introducing a 5.00 mm deep cut in the pipe surface. 90° wedges. 1.00 m distance. Spectrum smoothed to 1/32 octave bands.

The amplitude spectra from measurements with the transducers directly on the pipe are shown in Figure 21. In resemblance with the spectra from measurements with 30° wedges, these spectra are also formed by a composite of wave types. The numerous peaks that appear from 1 MHz and up, are a special property of these spectra. The peaks are really much narrower than they appear in the smoothed spectra, and seem to appear at the same frequencies after introducing the damage to the pipe. This could support the possible explanation that the peaks are formed by resonances in the pipe wall directly under the active transducer. The peaks seem to have a favourable effect, as the before/after values differ by as much as around 10 dB in several of them, whereas the difference is generally around 5 dB.

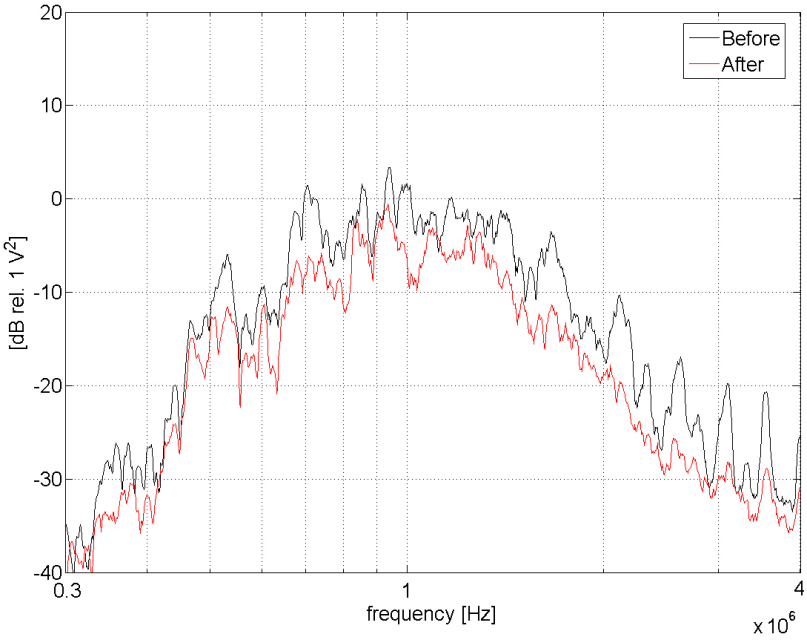

Figure 20: RMS-squared power density spectrum before/after introducing a 5.00 mm deep cut in the pipe surface. 30° wedges. 1.00 m distance. Spectrum smoothed to 1/32 octave bands.

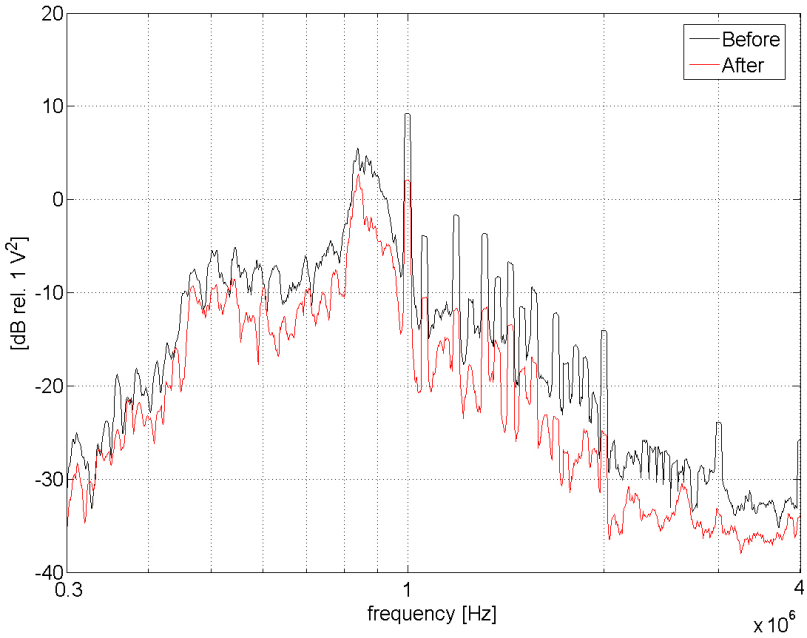

Figure 21: RMS-squared power density spectrum before/after introducing a 5.00 mm deep cut in the pipe surface. Transducers directly on pipe. 1.00 m distance. Spectrum smoothed to 1/32 octave bands.

4.3 Energy considerations

During the process of sawing into the pipe, one of the main motivations for performing a relatively high number of measurement with some of the wedges, was to get an idea of the degree of predictability. It was hoped that there would be a comprehensible dependency between the behaviour of the propagating signals and the size of the damage. As indicated also in Figure 15, this dependency turned out to be rather simple and predictable when measuring with 90° wedges. In a thesis such as this, it is unpractical, if not completely pointless to present plots from each of the 43 measurements performed with 90°, 70° and 60° wedges. However, knowing that the behaviours of the signals are dominated by decreasing amplitudes with growing damage size for all of these three wedge types, the total signal energy for each measurement can be used as a single descriptor. Figure 22 is a plot showing the sum of squared amplitudes as a function of the crack depth in the pipe surface. The measurement data is not scaled to any standard physical unit, but are still fully comparable with each other. The results are presented as the logarithm of the sum of squares. Even though the reference value is not very useful here, the unit is set to dB relative to 1 V^2s.

This plot shows that the energies are decreasing in a almost monotonous way as the depth of the cut in the pipe grows deeper. For the 90° wedges, the rapid decrease even with a crack of as little as $0.25 - 0.50$ mm in depth is very promising with respect to measurement sensitivity. On the other hand, all three graphs could have been approximated by straight lines and still be a fairly good model of the actual system. The reason why the 60° and 70° wedges give higher energy values for deeper depths of the crack than the 90° wedges, could be the second largest peaks in the envelopes. These peaks are not affected by the damage, and are larger with the 70° and 60° wedges, thus keeping the energy level higher as the main peak becomes relatively small.

If the energy is calculated from the signals arriving in the period $300 - 370$ μs only, the energy of the main burst only is taken into account. This changes the picture somewhat, but with the 90° wedges the change is very small. See Figure 23. However, for the 70° and 60° wedges, –especially the 60° wedges, the change is more interesting. Firstly, we see that the energy of the main burst follows a nearly linear trend for all three types of wedges for crack depths up to 3.00 mm. For deeper cuts, the decrease in energy seems to stop completely with the 60° wedges, whereas the 90° and 70° wedges keep following this decreasing trend until around 5.00 mm in depth. It is hard to tell why the waves from the 60° wedges behave so differently for depths of more than 3.00 mm, but perhaps would the transferred energy stop decreasing also with 90° and 70° wedges at a certain depth.

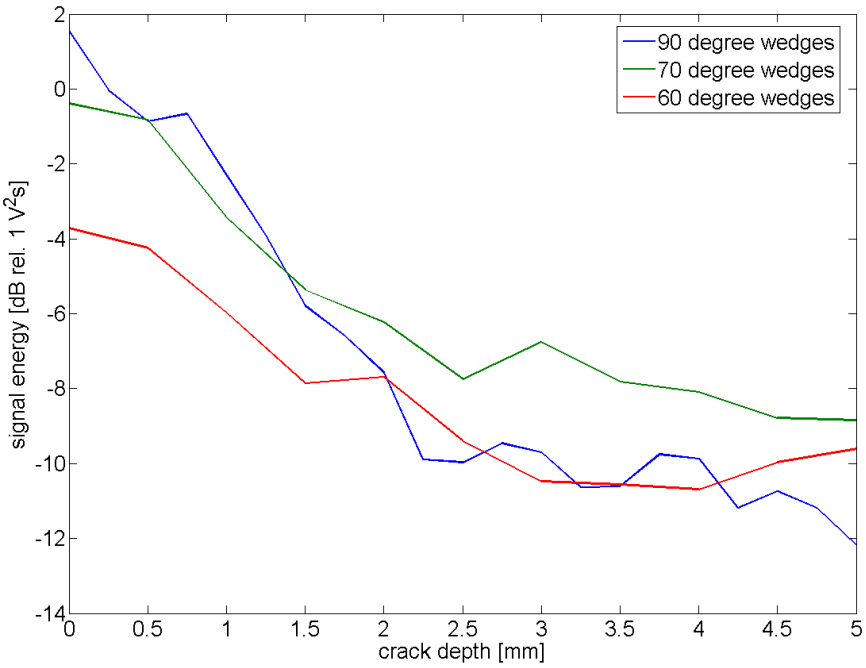

Figure 22: Transmitted signal energy as a function of pipe damage.

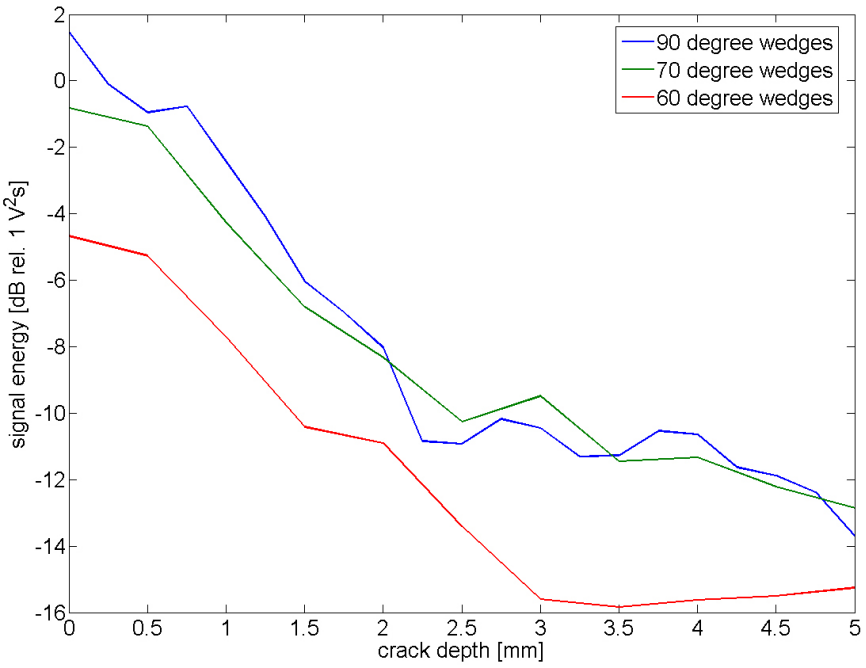

Figure 23: Transmitted signal energy as a function of pipe damage. Only energy of main burst from 300 to 370 µs included.

5 Conclusion

Through experimental work, it has been shown that even simple systems can be used to monitor the condition of steel pipes by the use of ultrasound. By using angle beam wedges, it is possible to introduce Rayleigh waves with strong amplitudes and good sensitivity to discontinuities. It is possible that these vibrations travel both directly between the transducers and around the perimeter of the pipe, thus potentially providing very useful information about the general condition of the pipe.

Measurement techniques using ultrasound gel, have been developed to achieve the degree of repeatability necessary in introductory lab measurements. However, the use of ultrasound gel is only recommended for introductory examinations or other situations where the transducers and wedges have to be moved around or changed frequently. For more in-depth studies or in the design of a commercial product, some form of glue should be used with custom wedges with curved contact surfaces.

Especially the time domain results from measurements with the 90° wedges for excitation of Rayleigh waves, were so simple that advanced signal processing was unnecessary. Nothing more than simple averaging and HP-filtering was used in any of the presented results. Tests with as much as 4.38 m distance between the wedges showed that usable signal-to-noise ratios could be attained by extensive averaging. With a more optimized measurement setup, it is possible that signal amplitudes could have been increased, and the number of averages could have been reduced accordingly.

Whether surface waves propagate equally well along a pipe surface wrapped in a protective plastic coating, is one of the questions that will have to be answered to find out if this wave type is applicable for sub sea pipelines. It was assumed that the plastic coating of these pipes have a much lower acoustic impedance than steel. Given that this assumption is correct, the presented results that describe Rayleigh waves, should give a good indication of the behaviour of this type of waves on a plastic wrapped pipe. For steel pipes without plastic coating, that are painted or have other surface treatments, the conditions for Rayleigh waves will be more or less changed depending on the surface treatment, but there is reason to believe that the presented results are representative to some of these conditions as well. Even in the worst case, if problems with the use of Rayleigh waves should occur, the results indicate that especially with some of the wedges or with transducers directly on the pipe, also longitudinal and shear waves could probably be used for monitoring of pipe stretches several meters long. These wave types are less dependent on the medium surrounding the pipe.

The predictable signal degradation caused by the cut in the surface, is indeed good news regarding possibilities for further development of a simple pipe monitoring system. Even with off-the-shelf equipment, and with limited knowledge about the theory of wave propagation in pipe walls, it was shown that a discontinuity could be detected and roughly sized. Even though the testing was conducted under somewhat idealized conditions with a single discontinuity right between the transducers, the results indicate that relatively simple systems for general condition monitoring of steel pipes can be made.

References

[Cartz 1995] Louis Cartz: *Nondestructive Testing,* ASM International, The Materials Information Society, Materials Park 1995

[Hinders 2002] Kevin R Leonard, Eugene V Malyarenko and Mark K Hinders: *Ultrasonic Lamb wave tomography,* Department of Applied Science, College of William and Mary, Williamsburg 2002

[Krautkrämer 1990] Josef Krautkrämer, Herbert Krautkrämer: *Ultrasonic Testing of Materials*, Springer-Verlag, Berlin, 1990

[Olympus 2006] Olympus - Panametrics-NDT: *Ultrasonic Transducers for Nondestructive Testing,* (UT Transducer catalog), Olympus, 2006

[Olsen 1992] Josef Olsen og Erik Rødsand: *Ikke-destruktiv materialprøving,* Teknologisk Institutt, 1992

[Persson 1993] Gert O.M. Persson: *Elastic Wave Scattering by Cracks,* Chalmers University of Technology, Gothenburg 1993

[SmartPipe] http://www.smartpipe.com – Website for the SmartPipe project, hosted by SINTEF, Trondheim, 2007

Appendix I: Measurement equipment

- Panametrics 5 MHz angle-beam transducers V543-SM, S/N: 155471, 155474
- Panametrics surface wave wedges: ABWML-4T-90°
- Panametrics Accupath wedges: ABWM-4T-X° (70°, 60°, 45° and 30° type wedges)
- Panametrics 1 MHz immersion-type transducers C302-SU, S/N: 517021, 517022
- Panametrics pulser receiver model 5052 PR, S/N: 1395
- Panametrics ultrasonic preamp S/N: 5676/1305
- Krohn-Hite Corp. Model 3945 IEEE-488 Programmable 3-Channel Tunable Active Filter, 3 Hz to 25 MHz, DB-2013
- LeCroy 9410 dual 150 MHz Oscilloscope, S/N: 2589, KA-4237
- DANE-GEL E2, aqueous transmission gel for electromedical procedures

Appendix II: Transducer datasheets

OLYMPUS

Tel: 781-419-3900
www.olympusndt.com

TRANSDUCER DESCRIPTION

PART NO.: V543
SERIAL NO.: 155474
DESIGNATION: CONTACT

FREQUENCY: 5.00 MHz
ELEMENT SIZE: .25 in. DIA.

TEST INSTRUMENTATION

PULSER/RECEIVER: PANAMETRICS 5052UA #1
DIGITAL OSCILLOSCOPE: LeCroy LT342 / SN: LT34202249
TEST PROGRAM: TP103-3 VER. 10738H
CABLE: RG 174/U LENGTH: 4FT

TEST CONDITIONS

PULSER SETTING: ENERGY: 1 ; DAMPING: 100 OHMS
RECEIVER SETTING: ATTN: 40dB ; GAIN: 40dB
TARGET: .5 IN. POLYSTYRENE
JOB CODE: TP200

MEASUREMENTS PER ASTM E1065

WAVEFORM DURATION:
-14DB LEVEL --- 0.228 US
-20DB LEVEL --- 0.344 US
-40DB LEVEL --- 0.716 US

SPECTRUM MEASURANDS:
CENTER FREQ. ------ 5.1 MHz
PEAK FREQUENCY -- 4.98 MH:
-6DB BANDWIDTH --- 131.08 %

COMMENTS:

** ACCEPTED

TECHNICIAN (3) Daniel Santoyo

DATE: 03-29-2007

SIGNAL WAVEFORM

(.2 USEC / DIVISION)

FREQUENCY SPECTRUM

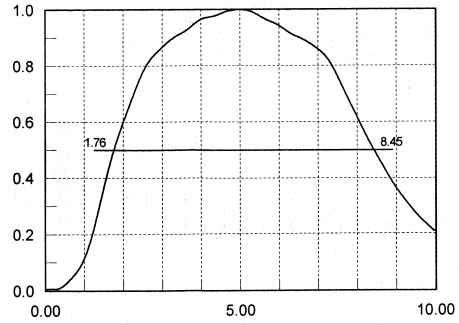

PANAMETRICS-NDT™

TP1XX Rev. A TEG Dwg# 16150

OLYMPUS

Tel: 781- 419-3900
www.olympusndt.com

TRANSDUCER DESCRIPTION

PART NO.: V543
SERIAL NO.: 155471
DESIGNATION: CONTACT

FREQUENCY: 5.00 MHz
ELEMENT SIZE: .25 in. DIA.

TEST INSTRUMENTATION

PULSER/RECEIVER: PANAMETRICS 5052UA #1
DIGITAL OSCILLOSCOPE: LeCroy LT342 / SN: LT34202249
TEST PROGRAM: TP103-3 VER. 10738H
CABLE: RG 174/U LENGTH: 4FT

TEST CONDITIONS

PULSER SETTING: ENERGY: 1 ; DAMPING: 100 OHMS
RECEIVER SETTING: ATTN: 40dB ; GAIN: 40dB
TARGET: .5 IN. POLYSTYRENE
JOB CODE: TP200

MEASUREMENTS PER ASTM E1065

WAVEFORM DURATION:
-14DB LEVEL --- 0.304 US
-20DB LEVEL --- 0.348 US
-40DB LEVEL --- 0.720 US

SPECTRUM MEASURANDS:
CENTER FREQ. ------ 4.98 MHz
PEAK FREQUENCY -- 4.04 MHz
-6DB BANDWIDTH --- 131.16 %

COMMENTS:

** ACCEPTED

TECHNICIAN (3) David Santiago

DATE: 03-29-2007

SIGNAL WAVEFORM

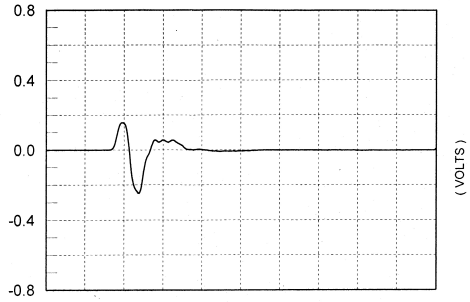

(.2 USEC / DIVISION)

FREQUENCY SPECTRUM

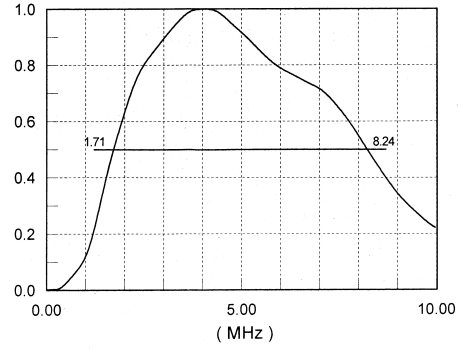

PANAMETRICS-NDT

TP1XX Rev. A TEG Dwg# 16150

BG-2021

PANAMETRICS-NDT
A Business of R/D Tech Instruments Inc.
Tel: 781-419-3900
www.panametrics-ndt.com

TRANSDUCER DESCRIPTION

PART NO.: C302
SERIAL NO.: 517021
DESIGNATION: FLAT IMMERSION
FREQUENCY: 1.00 MHz
ELEMENT SIZE: 1 in. DIA.

TEST INSTRUMENTATION

PULSER/RECEIVER: PANAMETRICS 5052UA #4
DIGITAL OSCILLOSCOPE: LeCroy LT262 / SN: LT26200531
TEST PROGRAM: TP103-3 VER. 1046UK
CABLE: RG-58 A/U LENGTH: 4FT

TEST CONDITIONS

PULSER SETTING: ENERGY: 1 ; DAMPING: 50 OHMS
RECEIVER SETTING: ATTN: 28dB ; GAIN: 20dB
TARGET: 2.0 IN SILICA
JOB CODE: TP200
WATER PATH: 1.005 in

MEASUREMENTS PER ASTM E1065

WAVEFORM DURATION:
-14DB LEVEL --- 1.660 US
-20DB LEVEL --- 1.840 US
-40DB LEVEL --- 3.440 US

SPECTRUM MEASURANDS:
CENTER FREQ. ------ 1.05 MHz
PEAK FREQUENCY -- 0.97 MHz
-6DB BANDWIDTH --- 82.07 %

COMMENTS:

F#: 1.04

** ACCEPTED

TECHNICIAN (99)

DATE: 03-07-2005

SIGNAL WAVEFORM

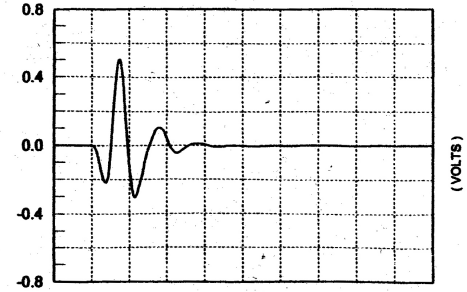

FREQUENCY SPECTRUM

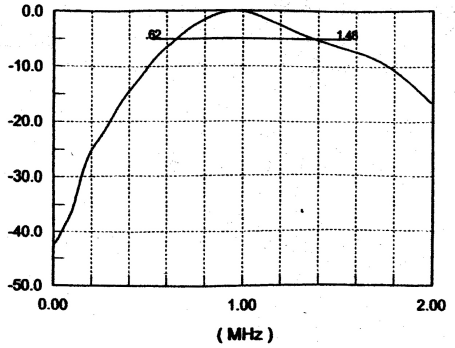

TP1XX Rev. A TEG Drwg# 16150

BG-2022

PANAMETRICS-NDT™

A Business of R/D Tech Instruments Inc.
Tel: 781- 419-3900
www.panametrics-ndt.com

TRANSDUCER DESCRIPTION

PART NO.: C302
SERIAL NO.: 517022
DESIGNATION: FLAT IMMERSION

FREQUENCY: 1.00 MHz
ELEMENT SIZE: 1 in. DIA.

TEST INSTRUMENTATION

PULSER/RECEIVER: PANAMETRICS 5052UA #4
DIGITAL OSCILLOSCOPE: LeCroy LT262 / SN: LT25200531
TEST PROGRAM: TP103-3 VER. 1049UK
CABLE: RG-58 A/U LENGTH: 4FT

TEST CONDITIONS

PULSER SETTING: ENERGY: 1 ; DAMPING: 50 OHMS
RECEIVER SETTING: ATTN: 26dB ; GAIN: 20dB
TARGET: 2.0 IN SILICA
JOB CODE: TP200

WATER PATH: 1.002 in

MEASUREMENTS PER ASTM E1065

WAVEFORM DURATION:
-14DB LEVEL --- 1.200 US
-20DB LEVEL --- 1.840 US
-40DB LEVEL --- 3.440 US

SPECTRUM MEASURANDS:
CENTER FREQ. ------ 1.04 MHz
PEAK FREQUENCY -- 0.96 MHz
-6DB BANDWIDTH --- 82.96 %

COMMENTS:

F#: 1.04

SIGNAL WAVEFORM

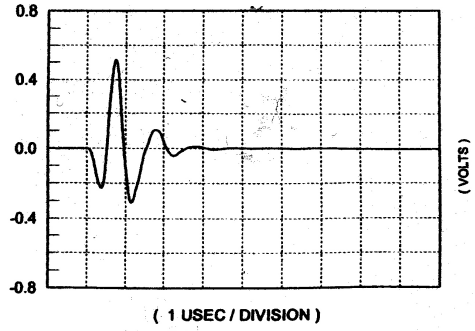

(1 USEC / DIVISION)

FREQUENCY SPECTRUM

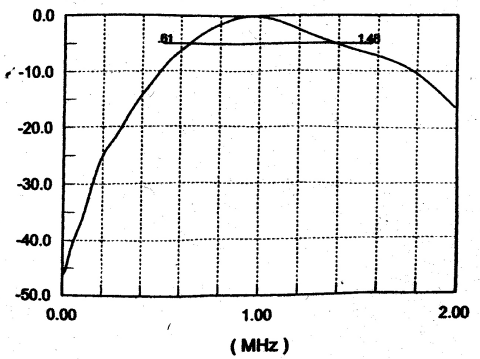

** ACCEPTED

TECHNICIAN (99)

DATE: 03-07-2005

TP1XX Rev. A TBS Drwg# 16150